

Critical investigation of the infrared-transmission-data analysis of hydrogenated amorphous silicon alloys

N. Maley

Coordinated Science Laboratory, University of Illinois, Urbana, Illinois 61801

(Received 10 October 1991; revised manuscript received 31 January 1992)

Infrared-transmission spectroscopy is widely used to obtain quantitative information about hydrogen bonding in hydrogenated amorphous silicon (a -Si:H), silicon-germanium (a -SiGe:H), and silicon-carbon (a -SiC:H) alloys. To simplify the conversion of transmission spectra to absorption spectra the most commonly used methods, suggested by Brodsky, Cardona, and Cuomo (BCC) [Phys. Rev. B **16**, 3556 (1977)] and Connell and Lewis (CL) [Phys. Status Solidi B **60**, 291 (1973)], assume incoherent multiple reflections in the film as well as the substrate. We show that the absorption in a -Si:H alloy films on c -Si substrates is different for coherent and incoherent reflections in the film. This difference causes the BCC and CL methods to overestimate or underestimate the absorption coefficient (α) in many experimental situations. The most notable feature is an overestimate of α if the film thickness d is below a critical value (d_{\min}). For $d > d_{\min}$, the error in absorption coefficient is usually less than 10%. Below d_{\min} , the error in α increases as d decreases. The maximum error, which occurs in the limit $d \rightarrow 0$, increases with the refractive index of the film and is $\geq 30\%$ for a -SiC:H alloys, $\sim 70\%$ for a -Si:H, and $\leq 90\%$ for a -SiGe:H alloys. The value of d_{\min} decreases as the refractive index of the film and the frequency of the vibrational mode increase. For a -Si:H, for example, the hydrogen content determined from the 640-cm^{-1} Si-H wagging-mode absorption is overestimated if d is less than $\sim 1\ \mu\text{m}$. We show that experimental data are consistent with the predictions of this analysis. In most cases it is possible to correct the results from the BCC and CL methods so that they are accurate to within 10%. For greater accuracy, infrared-transmission data should be analyzed by taking the effects of optical interference into account.

I. INTRODUCTION

The structural, optical, and electronic properties of hydrogenated amorphous silicon (a -Si:H), silicon-germanium (a -SiGe:H), and silicon-carbon (a -SiC:H) alloys are very sensitive to the hydrogen concentration C_H . Among the several techniques available to measure C_H , ir transmission is perhaps the most commonly used since it is nondestructive, fast, and convenient. In addition to C_H , it also provides information regarding the bonding configurations. The determination of C_H from ir data involves (i) the measurement of the transmission spectra $T(\omega)$ of thin films usually deposited on c -Si substrates, (ii) the conversion of $T(\omega)$ to absorption spectra $\alpha(\omega)$, and (iii) relating the integrated absorbances of various modes to bond concentrations using empirically determined oscillator strengths.^{1,2} We identify two sources of error in converting $T(\omega)$ to $\alpha(\omega)$, which in turn lead to errors in the determination of the oscillator strengths and/or hydrogen content.

The most commonly used method to convert $T(\omega)$ to $\alpha(\omega)$ is the one suggested by Brodsky, Cardona, and Cuomo (BCC).¹ A somewhat less common method is that of Connell and Lewis (CL).³ To simplify the data analysis, both methods assume incoherent multiple reflections in the film as well as the substrate, though this is usually not true for experimental data. In this paper we use the optical constants of a -Si:H, a -SiGe:H, and a -SiC:H alloys, take into account coherent multiple reflections in the film and incoherent multiple reflections in the substrate, and

calculate transmission spectra. Analyzing the simulated spectra by the BCC and CL methods shows that both methods systematically overestimate α for very thin films and over- or underestimate it by up to 10–20% for thicker films. The error is primarily a function of ωd , where ω is the vibrational frequency and d is the film thickness. The error also depends on the refractive index and absorption coefficient of the film and the refractive index of the substrate. Infrared-data analysis also involves estimating a baseline, i.e., removing the interference fringes from the transmission spectra. Uncertainty in estimating the baseline is another source of error in the BCC and CL methods, and it can affect the results of deconvoluting and integrating the absorption bands by 20% or more. In a previous paper we described the errors in the hydrogen content of a -Si:H determined from the 640-cm^{-1} wagging mode using the BCC method.⁴ In this paper we (i) examine the origin of the errors in the BCC and CL methods, (ii) quantify the errors at all vibrational frequencies for a -SiGe:H and a -SiC:H alloys as well as a -Si:H, and (iii) discuss some of the consequences. In most cases it is possible to correct the results from the two methods so that they are accurate to within 10%. For greater accuracy ir-transmission data should be analyzed by taking the effects of optical interference into account.

II. SIMULATIONS AND ANALYSIS

For the simulations we consider an absorbing film on a nonabsorbing substrate and light at normal incidence (see

Fig. 1). In reality, there is some absorption in the *c*-Si substrate at frequencies below $\sim 1200 \text{ cm}^{-1}$. Experimentally, this is taken into account by dividing the sample transmission by that of a bare substrate and multiplying by 0.54, the absorption-free transmission of *c*-Si. This assumes that absorption in the substrate is not modified by the presence of the film. The substrate also has thin layers ($\sim 20 \text{ \AA}$) of native oxide on both front and back, whose effect is ignored in the data analysis. Our simulations shows that these approximations affect the results by less than 5%. Hence, for simplicity, we assume the substrate is nonabsorbing and has no oxide layers.

We calculate the transmission T as a function of the vibrational frequency (ω), the refractive index of the substrate (n_3), the refractive index (n_2 or n), absorption coefficient (α_2 or α), and thickness of the film (d).⁵ The substrate is assumed to be optically thick so that multiple reflections in it are incoherent; i.e., we sum the intensities of the multiply reflected beams. We consider incoherent multiple reflections in the film to derive the BCC and CL equations and coherent multiple reflections to simulate experimental data.

We first consider a thin film on a semi-infinite substrate. In the incoherent limit, by summing the intensities of the multiply reflected beams, we get

$$T_{13} = T_{12} T_{23} e^{-\alpha d} / (1 - R_{23} R_{21} e^{-2\alpha d}), \quad (1a)$$

$$R_{13} = R_{12} + T_{12} T_{21} R_{23} e^{-2\alpha d} / (1 - R_{23} R_{21} e^{-2\alpha d}), \quad (1b)$$

and

$$R_{31} = R_{32} + T_{32} T_{23} R_{21} e^{-2\alpha d} / (1 - R_{23} R_{21} e^{-2\alpha d}). \quad (1c)$$

In the coherent limit, by summing the electric fields of the multiply reflected beams, we get

$$T_{13} = (n_3/n_1) |t_{12} t_{23} P / (1 - P^2 r_{21} r_{23})|^2, \quad (2a)$$

$$R_{13} = |r_{12} + P^2 t_{12} t_{21} r_{23} / (1 - P^2 r_{21} r_{23})|^2, \quad (2b)$$

and

$$R_{31} = |r_{32} + P^2 t_{32} t_{23} r_{21} / (1 - P^2 r_{21} r_{23})|^2. \quad (2c)$$

In Eqs. (1) and (2), for $j = i \pm 1$, we have

$$t_{ij} = 2N_i / (N_i + N_j), \quad (3a)$$

$$r_{ij} = (N_i - N_j) / (N_i + N_j), \quad (3b)$$

$$R_{ij} = |r_{ij}|^2, \quad (3c)$$

$$T = \frac{(1 - R_{12})(1 - R_{23})(1 - R_{34})e^{-\alpha d}}{(1 - R_{23}R_{34}) - (R_{12}R_{23} + R_{12}R_{34} - 2R_{12}R_{23}R_{34})e^{-2\alpha d}}. \quad (5)$$

The Connell-Lewis method uses Eq. (5) and an independent measurement of n to determine α .^{3,6} The refractive index, for example, can be determined by combining profilometric measurements of film thickness with fringe spacing in reflectance spectra for films on glass. The BCC method simplifies the data analysis further by

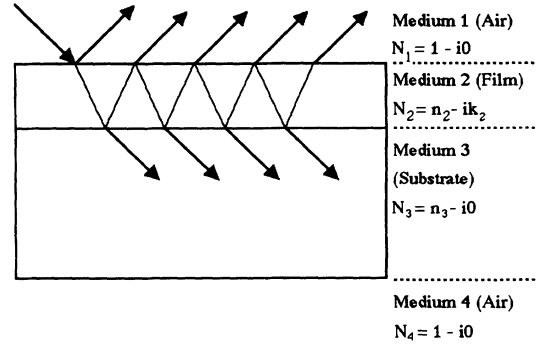


FIG. 1. Schematic of a thin film on a substrate. Multiple reflections in the substrate are omitted, and light is shown at a non-normal angle of incidence for clarity.

$$T_{ij} = n_j / n_i |t_{ij}|^2, \quad (3d)$$

and

$$P = \exp(-2\pi i N_2 d \omega). \quad (3e)$$

Here N_i , the complex refractive index of medium i , is equal to $n_i - ik_i$ and the extinction coefficient k_i is related to the absorption coefficient α_i via $\alpha_i = 4\pi k_i \omega$. The quantities T_{13} and R_{13} represent the transmission and reflectance of a film on a semi-infinite substrate for light incident from the air side and R_{31} is the reflectance for light incident from the substrate side. (Note that $T_{31} = T_{13}$, but $R_{31} \neq R_{13}$.)

The equations for a thin film on a substrate of finite thickness are derived by considering a structure whose front-surface reflectance and transmission are those of the film on a semi-infinite substrate and whose back-surface reflectance and transmission are those of the substrate-air interface. To do this we replace R_{12} , T_{12} , R_{21} , T_{21} , R_{23} , T_{23} , and R_{32} , in Eqs. (1) by R_{13} , T_{13} , R_{31} , T_{31} , R_{34} , T_{34} , and R_{43} , respectively. We also replace α_2 by α_3 ($=0$ since the substrate is nonabsorbing). With these substitutions we get

$$T = T_{34} T_{13} / (1 - R_{31} R_{34}), \quad (4)$$

where T_{13} and R_{31} are given, respectively, by Eqs. (1) and (2) for incoherent and coherent multiple reflections in the film. In the incoherent limit, Eq. (5) can be further simplified to give

assuming that the difference in the real part of the refractive index between the film (n_2) and the substrate ($n_3 = 3.42$) is negligible and that there are no reflections at the film-substrate interface.¹ Thus setting $R_{12} = R_{34}$ and $R_{23} = 0$ in Eq. (5) gives

$$T = (1 - R_{12})^2 e^{-\alpha d} / (1 - R_{12}^2 e^{-2\alpha d}). \quad (6)$$

This can be rewritten as

$$T = 4T_{\text{NA}}^2 e^{-\alpha d} / [(1 + T_{\text{NA}})^2 - (1 - T_{\text{NA}})^2 e^{-2\alpha d}], \quad (7)$$

where T_{NA} is the baseline transmission when the film is nonabsorbing. If the film refractive index is indeed equal to that of the substrate, as is assumed in the BCC method, then $T_{\text{NA}} = T_S = 0.54$, the absorption-free transmission of *c*-Si. However, as we will see in the next section, the refractive index of *a*-Si:H is a function of hydrogen content and can deviate from the crystalline value of 3.42 by $\pm 10\%$. For *a*-SiGe:H and *a*-SiC:H, the refractive index is a function of composition and can range from less than 2.5 (carbon-rich alloys) to ~ 4.0 (Ge-rich alloys).^{7,8} Because of the index mismatch at the film-substrate interface, T_{NA} in Eq. (7) is different from the bare substrate transmission. However, *a*-Si:H is nonabsorbing in most of the spectral region of interest. Hence the baseline for the absorption bands can, in principle, be determined by interpolating the transmission from adjacent nonabsorbing regions. This should be done with some caution for the 640-cm^{-1} Si-H wagging mode, as there is some absorption below 550-cm^{-1} due to Si-Si bonds.⁹ Since most ir spectrometers measure spectra at frequencies above 400-cm^{-1} , we do not, in general, have transmission at frequencies below the 640-cm^{-1} band corresponding to nonabsorbing regions.

Problems with baseline estimation are eliminated when exact equations are used to analyze ir data. By setting α and k equal to zero in Eqs. (2)–(4), we can calculate T_{NA} exactly. Figure 2 shows typical experimentally measured transmission spectra of *a*-Si:H and *a*-SiC:H films (after correcting for absorption in the *c*-Si substrate). Also shown in the figure are the baselines calculated by optimizing n and d . The procedure is quite straightforward as the period of the fringes depends on the product nd and the amplitude on n or, more precisely, the mismatch in index between the film and substrate. In most cases we

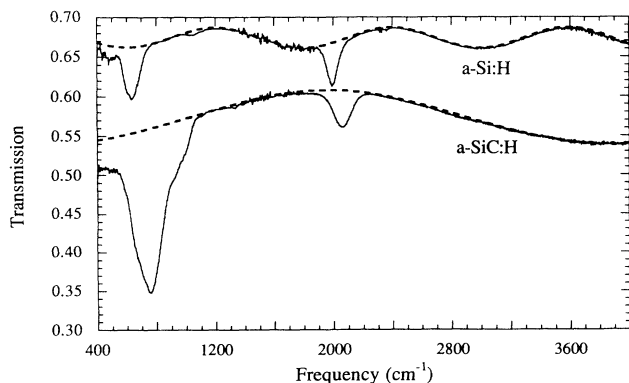


FIG. 2. Transmission spectra of *a*-Si:H (upper curve) and *a*-SiC:H (lower curve) films corrected for absorption in the *c*-Si substrate. The *a*-Si:H spectrum has been shifted vertically by 0.15. Dashed lines show the baseline fit to the nonabsorbing regions.

can obtain a good baseline using a constant value of refractive index for the entire spectral range.

In Fig. 2 we can clearly see the Si-Si stretching mode at $\sim 500\text{-cm}^{-1}$. If this peak is not taken into account in estimating the baseline, the integrated area of the 640-cm^{-1} peak would be underestimated by 15–20%. Figure 2 also shows that the Si-Si mode is stronger in the *a*-SiC:H film. This occurs because of the enhancement of the Si-Si bond absorption strength in the presence of carbon.¹⁰ In *a*-SiGe:H alloys, the Si-Si stretching mode overlaps with the Ge-H wagging mode¹¹ at 565-cm^{-1} . Failure to take the Si-Si band into account can thus lead to errors in integrating the H-related bands in alloys also. From Fig. 2 we can also see that using the bare substrate transmission as the baseline ($T_{\text{NA}} = 0.54$ for the entire spectrum) in the BCC analysis is clearly inappropriate as it fails to account for the interference fringes. We do not even know if this is a common practice since most authors do not describe the details of their data analysis. We will not address the consequences of this choice except to note that the errors resulting from it are much larger than the ones described in the next section.

The analytical determination of T_{NA} has the additional advantage that all the information required to analyze the ir data is obtained from a single measurement on a single sample. It also avoids errors which can arise from using transmission and thickness measurements made on different parts of a sample (if film thickness is not uniform over large areas). However, calculating a baseline using Eqs. (2)–(4) does require that the film thickness be uniform over the area (typically a few mm^2) where transmission is measured. Determining d from fitting the baseline is also difficult if the film refractive index is very close to that of the substrate as the amplitude of the fringes depends on the index mismatch.

A third advantage of the analytic determination of the baseline is that it improves the accuracy of deconvoluting overlapping peaks. This is particularly useful for separating the Si-H stretching modes at 2000 and 2100-cm^{-1} and for *a*-SiC:H alloys, where several Si-Si, Si-H, Si-C, and C-H related peaks appear at frequencies below 1000-cm^{-1} .¹²

For the results presented in the next section, we assume coherent multiple reflections in the film and calculate T and T_{NA} using exact equations and optical constants appropriate for *a*-Si:H, *a*-SiGe:H, and *a*-SiC:H. We then analyze the data by the BCC and CL methods. It is easy to see from Eq. (5) that the absorption spectra obtained from T alone by the CL method contain interference fringes. To correct for this we compute α from both T and T_{NA} and take the difference. We have also noted earlier that the BCC equation [Eq. (7)] is derived from the CL equation [Eq. (5)] by neglecting reflections at the film-substrate interface. However, using a baseline that is different from the bare substrate transmission partially accounts for reflections at this interface. As a consequence, we will see in the next section that results from the two methods usually differ by less than 10%.

To assess the relevance of the present simulations to actual measurements, we need to know when the

coherent and incoherent limits are valid. Reflections in the film and substrate can be coherent or incoherent, depending on their thickness, the flatness and parallelism of the interfaces, and the instrumental resolution. Coherent reflections in *c*-Si substrates, which are typically 0.5 mm thick, can be eliminated by decreasing the instrumental resolution to 4 cm^{-1} or less or by using wedged or roughened substrates. Since most *a*-Si:H films are only a few micrometers thick, coherent reflections in them can only be eliminated if the films are deposited on rough surfaces. Since ir absorption in *a*-Si:H is at wavelengths between 4.5 and $20 \mu\text{m}$, the substrate surface must be considerably rough, particularly for the longer wavelengths.

III. RESULTS

It is common knowledge that reflection and transmission of a thin film are not the same in the coherent and incoherent limits. Although less obvious, the absorbance of the film ($A = 1 - R - T$) is different in the two limits. Figure 3 shows A_{coh} and A_{incoh} as a function of thickness for a free-standing film with $n = 3.0$, $\omega = 640 \text{ cm}^{-1}$, and $k = 0.25$ ($\alpha = 2000 \text{ cm}^{-1}$). In the incoherent limit absorption in the film increases monotonically with thickness. On the other hand, Fig. 3 shows that A_{coh} is very nonmonotonic; it is nearly constant for d between 0.5 and $1.5 \mu\text{m}$ and is greater for $d = 2.7 \mu\text{m}$ than for thicker films. In the coherent limit the phase difference between multiply reflected beams changes with thickness and interference between these beams leads to periodic changes in the distribution of the electric field and absorption in the film.

The difference between A_{coh} and A_{incoh} is, in general, a function of n , k , and ωd . Figure 4 shows the dependence of the ratio $A_{\text{coh}}/A_{\text{incoh}}$ on the quantity $2\pi n d \omega$ for $k = 0.25$ and $n = 2.0, 3.0$, and 4.0 . Figure 4 shows that even for relatively large values of $2\pi n d \omega$ (i.e., relatively thick films for infrared frequencies), A_{coh} is larger or smaller than A_{incoh} by as much as 50%. This difference can be quite important when dealing with free-standing films. Figure 4 also shows that, in the limit d (or ω) $\rightarrow 0$,

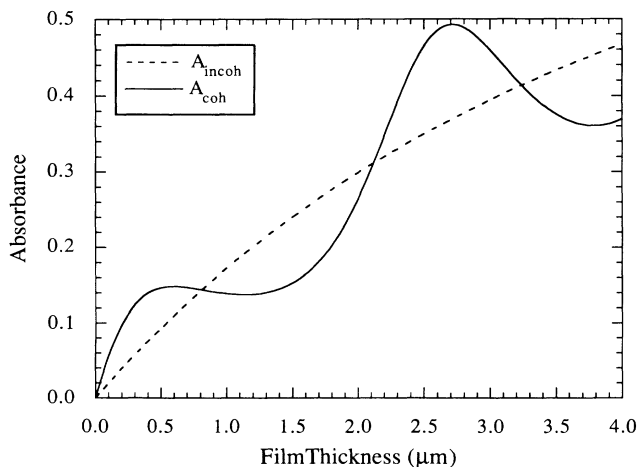


FIG. 3. Comparison of absorbance in a free-standing thin film in the coherent and incoherent limits.

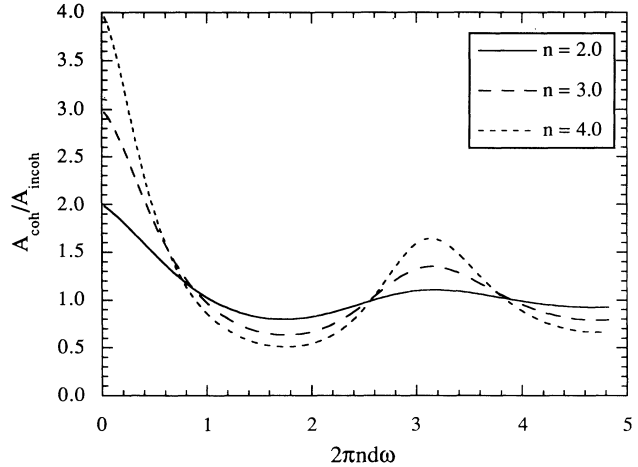


FIG. 4. Ratio of absorbance of a free-standing film in the coherent and incoherent limits shown as a function of the refractive index and product $2\pi n d \omega$.

A_{coh} is 2–4 times larger than A_{incoh} . The dependence of $A_{\text{coh}}/A_{\text{incoh}}$ on n in the limit $\omega d \rightarrow 0$ can be explained easily. In the incoherent limit, as n increases, more of the incident light is reflected at the front surface and absorption in the film decreases. In the coherent limit the electric field in the film is determined by the refractive index of the incident and transmission media, and the intensity of light and absorption in the film increase with n .⁵

For thin films on substrates, the difference between A_{coh} and A_{incoh} is qualitatively similar to that in Fig. 4 with the quantitative details depending on the refractive index of the substrate and on whether the substrate is semi-infinite or finite. This difference between A_{coh} and A_{incoh} leads to the BCC and CL methods over- or underestimating the absorption coefficient when analyzing experimental data. We denote the absorption coefficients calculated by the two methods by α_{BCC} and α_{CL} and show in Figs. 5–8 the dependence of $\alpha_{\text{BCC}}/\alpha$ and $\alpha_{\text{CL}}/\alpha$ on n , k , and ωd . As noted earlier, the values of n (2.5, 3.0, 3.5, and 4.0) cover the range that is of interest for *a*-SiC:H, *a*-Si:H, and *a*-SiGe:H alloys. For each n we use $k = 0.02$ and 0.5 to represent strong or weak absorption and vary ωd from 0 to 0.35. For the 640-cm^{-1} mode, this corresponds to d between 0 and $5 \mu\text{m}$, which is adequate for most purposes.

Figures 5–8 reveal several interesting features. First, as expected, α_{BCC} and α_{CL} are periodic in ωd . Second, the dependence of $\alpha_{\text{BCC}}/\alpha$ and $\alpha_{\text{CL}}/\alpha$ on n is relatively strong and the dependence on k is relatively weak. This is due to the fact that absorption increases with k both in the coherent and incoherent limits, while, as noted earlier, A_{coh} increases and A_{incoh} decreases with increasing n . Figures 5–8 also show that for the range of parameters explored, α_{BCC} and α_{CL} differ by 10% at most. (Since the two methods yield very similar results, in the remainder of this paper we will refer only to the more frequently used BCC method with the understanding that the comments apply to both methods.) Figures 5–8 show that the BCC method is accurate to within 10% for most

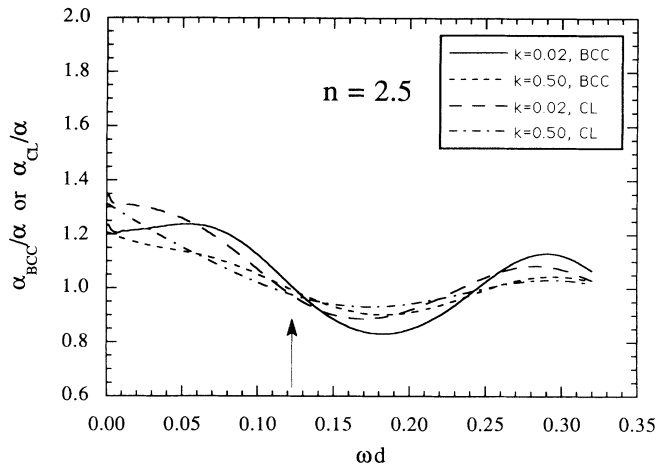


FIG. 5. Absorption coefficient determined by the BCC and CL methods normalized to the true α and shown as a function of the extinction coefficient and ωd product. The refractive index of the substrate, assumed to be nonabsorbing, is 3.42. The film refractive index is 2.5. The vertical arrow shows the value of $(\omega d)_{\text{min}}$.

values of ωd . However, with decreasing film thickness, it yields very misleading results as, depending on n , it overestimates the absorption coefficient by as much as 30–90%. In Figs. 4–8 we see that $\alpha_{\text{BCC}}/\alpha$ is considerably smaller than $A_{\text{coh}}/A_{\text{incoh}}$ in the limit $d \rightarrow 0$. This difference is due to the fact that in Fig. 4 we considered a free-standing film and in Figs. 5–8 the substrate is *c*-Si. In general, the error in $\alpha_{\text{BCC}}/\alpha$ is larger for substrates with lower refractive index (KBr or sapphire, for example).

The ωd dependence of α_{BCC} can somewhat arbitrarily be divided into two regimes. For $\omega d = (\omega d)_{\text{min}}$, $\alpha_{\text{BCC}} = \alpha$. For smaller ωd , the error increases as ωd decreases. For $\omega d > (\omega d)_{\text{min}}$, α_{BCC} is accurate to within 10% in most cases. If we take $\omega = 640 \text{ cm}^{-1}$ as an example, Figs. 5–8 show that d_{min} ranges from 0.8 μm for Ge alloys to 1.8

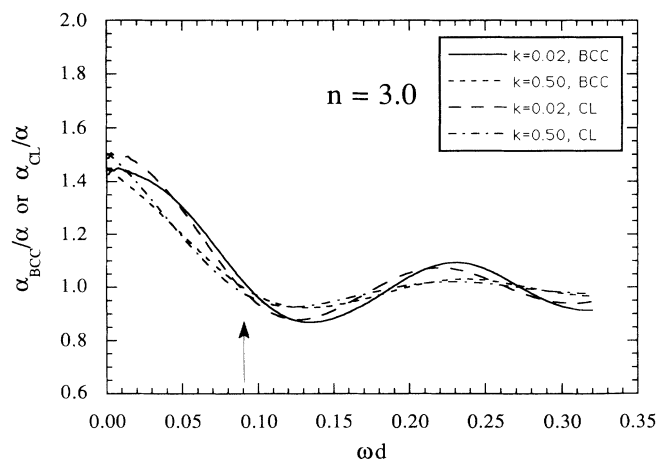


FIG. 6. Same as Fig. 5 except the film refractive index is 3.0.

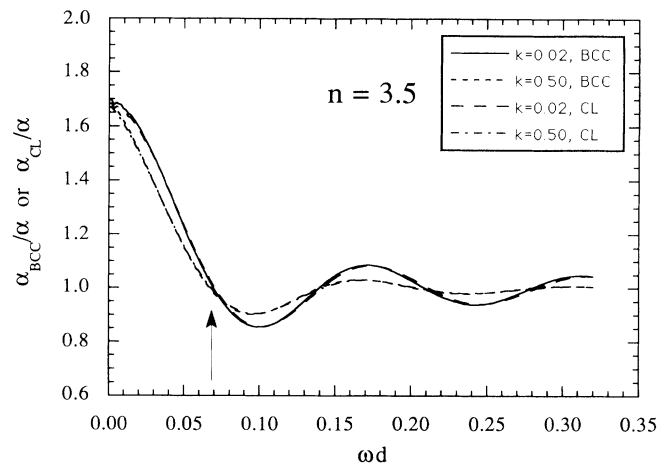


FIG. 7. Same as Fig. 5 except the film refractive index is 3.5.

μm for C alloys. Since these values are comparable to the thickness of *a*-Si:H and alloy films used in many studies, quantifying the errors in hydrogen content determined by the BCC method is quite important.

In the case of *a*-Si:H, it is possible to define a thickness-dependent correction factor. We have measured hydrogen content by thermal evolution and nuclear reactions and correlated it with infrared spectra for several *a*-Si:H films grown by magnetron sputtering and glow discharge.^{13,14} Figure 9 shows the dependence of n and k at 640 cm^{-1} on the hydrogen content. Using the linear dependence of n and k on C_{H} shown in Fig. 9, we have calculated $\alpha_{\text{BCC}}/\alpha$ for $C_{\text{H}} = 1, 5, 10, 15, 20, 25,$ and $30 \text{ at. } \%$. From the results, shown in Fig. 10, it is clear that for *a*-Si:H the error in α_{BCC} is primarily a function of ωd . The true absorption coefficient α can thus be obtained from α_{BCC} using the approximation

$$\alpha = \alpha_{\text{BCC}} / (1.72 - 12\omega d) \quad \text{for } \omega d \leq 0.06 \quad (8a)$$

and

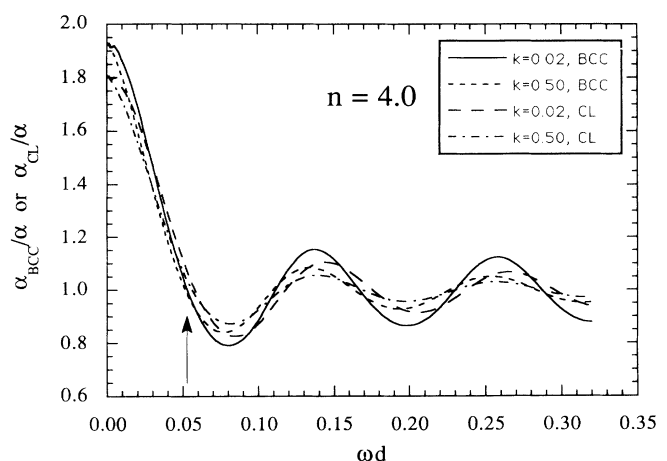


FIG. 8. Same as Fig. 5 except the film refractive index is 4.0.

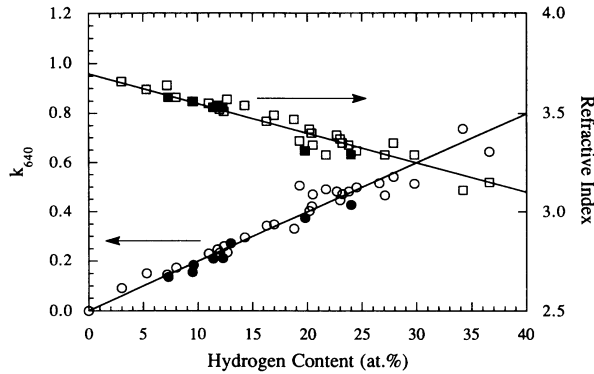


FIG. 9. Refractive index (squares) and the extinction coefficient at 640 cm^{-1} (circles) as a function of the hydrogen content of $a\text{-Si:H}$. Open symbols are for magnetron-sputtered films (Refs. 13 and 14), and solid symbols are for glow discharge (Ref. 14).

$$\alpha = \alpha_{\text{BCC}} \quad \text{for } \omega d \geq 0.06. \quad (8b)$$

These equations are a generalization of the correction factor for the wagging mode given in Ref. 4. Since the dependence of $\alpha_{\text{BCC}}/\alpha$ on k is relatively weak (Figs. 5–8), Eqs. (8) are applicable to all modes, even though the curves in Fig. 10 have been obtained using the k values of the wagging mode. The error in α obtained from Eqs. (8) is less than 10% in most of the cases, although it can be as much as 20% for certain values of ωd . The accuracy of ir-data analysis can be improved by using exact equations. The use of Eqs. (2)–(4) in determining the base line for transmission spectra has already been described in Sec. II. Since the wagging and stretching modes are usually fit to Gaussian peaks, it is relatively straightforward to use Eqs. (2)–(4) and calculate transmission spectra for an absorbing film—we need to specify film thickness and refractive index and position, height, and width of each Gaussian absorption band. Standard iterative procedures such as the Newton method can then be used to optimize these parameters by

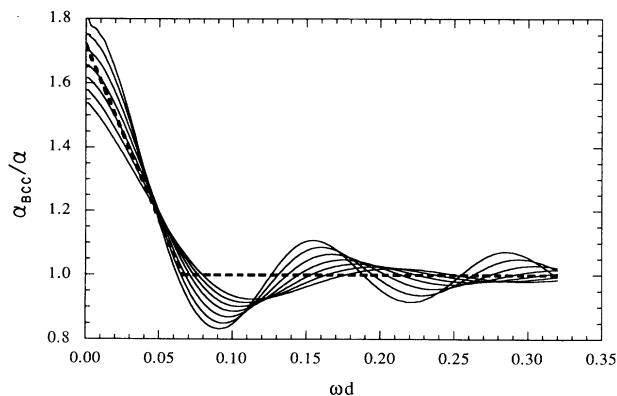


FIG. 10. Dependence of $\alpha_{\text{BCC}}/\alpha$ on the product ωd . Going from top to bottom at $d = 0$, the curves are for $C_{\text{H}} = 1, 5, 10, 15, 20, 25,$ and 30 at. %. The optical constants necessary for the simulations were obtained from Fig. 9. The dashed line represents Eq. (8).

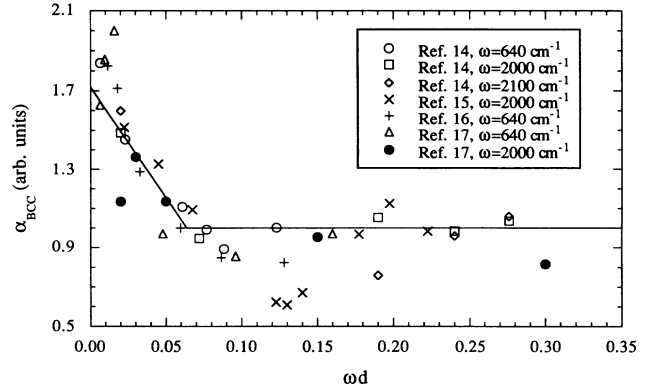


FIG. 11. Experimental data for the thickness dependence of α_{BCC} at $640, 2000,$ and 2100 cm^{-1} compared with the simplified linear dependence predicted by Eq. (8).

matching the calculated and measured transmission spectra.

In Fig. 11 we compare the predicted thickness dependence of Eq. (8) with available experimental data for both the Si-H wagging and stretching modes.^{14–17} Note that the ωd values represent film thicknesses up to $5.5\text{ }\mu\text{m}$ for the wagging mode and $1.75\text{ }\mu\text{m}$ for the stretching modes. Some of these experimental results have previously been attributed to hydrogen-rich interfacial layers which are thousands of angstroms thick.^{15,16} No satisfactory explanation has been available until now for the fact that this does not agree with trends in hydrogen content measured by other techniques.^{15,18} Figure 11 shows that the experimental data are in excellent agreement with Eq. (8) and that the apparent increase in hydrogen content is an artifact of the BCC analysis. Note that some of the scatter may be due to the uncertainty in estimating the base line for some of these data. Recent *ex situ*¹⁹ and *in situ*^{20–22} infrared-reflectance measurements on very thin films of $a\text{-Si:H}$ confirm that the trends seen in transmission data are an artifact, as they show that the hydrogen-rich surface layer is only $10\text{--}15\text{ \AA}$ thick.

IV. DISCUSSION

We have noted earlier that the BCC and CL methods under- or overestimate α because absorbance in a thin film is different for coherent and incoherent reflections in the film. The most surprising aspect of the results presented here is the magnitude of the error in the limit $d \rightarrow 0$ particularly for $a\text{-Si:H}$, where the refractive-index mismatch and hence reflection at the film-substrate interface are expected to be small. In fact, Fig. 9 shows that even when the film and substrate indices are equal, the BCC method overestimates α by $\sim 70\%$. There are three factors which contribute to this behavior. If we consider a thin film on a semi-infinite substrate, even if there is no mismatch in the real part of the refractive index at the film-substrate interface, the mismatch in the imaginary part leads to multiple reflections in the film and a difference in absorbance in the coherent and incoherent limits. In a practical geometry, reflections from the

substrate-air interface enhance this effect. Finally, measuring transmission alone, i.e., not taking into account the difference in reflectance in the coherent and incoherent limits, also leads to errors in α .

The errors in the BCC and CL methods have several important implications. They can introduce spurious trends in the variation of C_H as a function of any deposition parameters that affect the growth rate significantly. Plasma power and gas composition in glow-discharge deposition, power and target-substrate distance in sputtering, and substrate bias are some examples of such variables. In such studies, unless the deposition time is adjusted properly, the thickness for a series of films can vary systematically by a factor of 2 or 3 as the deposition variable is changed. From the preceding discussion we see that artifacts introduced by the analysis can enhance or suppress real trends or even produce spurious trends, particularly if d is less than d_{\min} for some of the films.

The errors in ir-data analysis may also explain the reported variation in A_{640} , the proportionality factor between hydrogen content, and the integrated absorbance of the 640-cm^{-1} Si-H wagging mode. The estimates for A_{640} range from a low of $1.6 \times 10^{19} \text{ cm}^{-2}$ (Refs. 2, 23, and 24) to a high of $2.5 \times 10^{19} \text{ cm}^{-2}$ (Ref. 25), with the former being the most commonly used value. Both values have been obtained by calibrating ir (sensitive to Si-H bonds) against techniques measuring the total hydrogen content. However, since the amount of molecular hydrogen in $a\text{-Si:H}$ is usually less than 1 at.%,^{26,27} it is unlikely that this difference is due to ir-inactive hydrogen. Recently, using the data-reduction procedures described in this paper, Langford *et al.*¹⁴ obtained $A_{640} = 2.1 \times 10^{19} \text{ cm}^{-2}$, which is in good agreement with the value of $2.0 \times 10^{19} \text{ cm}^{-2}$ reported by Maley *et al.*¹³ If we accept the latest measurement of A_{640} , then the earlier values differ from it by 20–25%, which is within the measurement uncertainty unless the systematic errors described in this paper are eliminated. For example, the films used in Ref. 24 are $\sim 0.6 \mu\text{m}$ thick and making the necessary thickness-dependent correction to α brings A_{640} from that study into closer agreement with Ref. 14. This issue is discussed in greater detail in Ref. 14.

The errors in the BCC method may also affect the comparison of the intensities of peaks at different frequencies. For example, in $a\text{-Si:H}$, thickness- and frequency-dependent effects can lead to different results for the hydrogen content determined from the wagging mode at 640 cm^{-1} and the stretching modes at 2000 and 2100 cm^{-1} .¹⁴ As another example, in $a\text{-Si:H}$, the 2100-cm^{-1} peak is attributed to Si-H stretching in dihydrides (SiH_2) and clustered monohydrides (SiH), and a doublet at $840\text{--}890 \text{ cm}^{-1}$ is attributed to the bending modes of dihydrides.²⁸ The dihydride and clustered monohydride concentrations can be determined by comparing the in-

tensities of these peaks.²⁹ However, the overestimate of α will persist to larger thicknesses for the lower-frequency mode and can lead to an underestimate of the clustered monohydride content. Another instance where comparing peak intensities might be relevant is in $a\text{-SiC:H}$ alloys. In this case the amount of H bonded to Si and C can, in principle, be determined from the Si-H and C-H stretching modes (at ~ 2000 and 2900 cm^{-1} , respectively).¹²

We have limited our analysis to $c\text{-Si}$ substrates and films with refractive index between 2.5 and 4.0. We have noted earlier that the errors in α_{BCC} and α_{CL} are larger for low-refractive-index substrates. Also, the refractive index can be less than 2.5 for carbon-rich $a\text{-SiC:H}$ alloys and dielectrics such as silicon nitride, silicon oxide, and oxynitrides.^{7,30} In such samples the BCC and CL methods can over- or underestimate α by up to 25% even for films that are several micrometers thick.

V. SUMMARY

In summary, the Brodsky-Cardona-Cuomo and Connell-Lewis methods assume incoherent multiple reflections in both the film and substrate to simplify the infrared-transmission-data analysis for $a\text{-Si:H}$, $a\text{-SiC:H}$, and $a\text{-SiGe:H}$ films. However, in most experimental situations, multiple reflections in the film are coherent. Differences in absorbance in the coherent and incoherent limits lead to the two methods over- or underestimating the absorption coefficient. Uncertainties in estimating the baseline for transmission spectra can also be a significant source of error in ir-data analysis. We have shown that the BCC and CL methods are equivalent and quantified the errors in them as a function of vibrational frequency, film thickness, and optical constants. For $a\text{-Si:H}$ the absorption coefficients determined by these methods can be corrected to within 10% in most cases by using a film thickness and frequency-dependent correction factor. For greater accuracy optical interference effects should be taken into account in the data analysis. Experimental data are shown to be in very good agreement with the predictions of the analysis. Finally, common experimental situations where the artifacts of the BCC method can lead to erroneous results are pointed out.

ACKNOWLEDGMENTS

This work has been funded by the Thin film Solar Cell Program of the Electric Power Research Institute under Contract No. EPRI RP 8001-7. The author would like to thank Dr. Igor Szafranek and Dr. Alison Langford for their help and many stimulating discussions.

¹M. H. Brodsky, M. Cardona, and J. J. Cuomo, *Phys. Rev. B* **16**, 3556 (1977).

²C. J. Fang, K. J. Gruntz, L. Ley, M. Cardona, F. J. Demond, G. Müller, and S. Kalbitzer, *J. Non-Cryst. Solids* **35&36**, 255

(1980).

³G. A. N. Connell and A. Lewis, *Phys. Status Solidi B* **60**, 291 (1973).

⁴N. Maley and I. Szafranek, in *Amorphous Silicon Technology*,

- edited by P. C. Taylor, M. J. Thompson, P. G. LeComber, Y. Hamakawa, and A. Madan, MRS Symp. Proc. No. 192 (Materials Research Society, Pittsburgh, 1990), p. 663.
- ⁵H. A. MacLeod, *Thin Film Optical Filters*, 2nd ed. (Hilger, Bristol, 1986).
- ⁶E. C. Freeman and W. Paul, *Phys. Rev. B* **18**, 4288 (1978).
- ⁷A. Matsuda, T. Yamaoka, S. Wolff, M. Koyama, Y. Imanishi, H. Kataoka, H. Matsuura, and K. Tanaka, *Appl. Phys. Lett.* **60**, 4025 (1986).
- ⁸S. Tsuda, H. Haku, H. Tarui, T. Matsuyama, K. Sayama, Y. Nakashima, S. Nakano, M. Ohnishi, and Y. Kuwano, in *Amorphous Silicon Semiconductors—Pure and Hydrogenated*, edited by A. Madan, M. J. Thompson, D. Adler, and Y. Hamakawa, MRS Symp. Proc. No. 95 (Materials Research Society, Pittsburgh, 1987), p. 311.
- ⁹S. C. Shen, C. J. Fang, M. Cardona, and L. Genzel, *Phys. Rev. B* **22**, 2913 (1980).
- ¹⁰N. Maley (unpublished).
- ¹¹G. A. N. Connell and J. R. Pawlik, *Phys. Rev. B* **13**, 787 (1976).
- ¹²H. Wieder, M. Cardona, and C. R. Guarnieri, *Phys. Status Solidi B* **92**, 99 (1979).
- ¹³N. Maley, A. Myers, M. Pinarbasi, D. Leet, J. R. Abelson, and J. A. Thornton, *J. Vac. Sci. Technol. A* **7**, 1267 (1989).
- ¹⁴A. A. Langford, M. L. Fleet, B. P. Nelson, W. A. Lanford, and N. Maley, *Phys. Rev. B* **45**, 13 367 (1992).
- ¹⁵J. Currie, F. Depelsenaire, S. Galarneau, J. Lecuyer, R. Groleau, J. Bruyere, and A. Deneuille, *J. Phys. (Paris)* **42**, L373 (1981).
- ¹⁶S. Hasegawa and Y. Imai, *Philos. Mag. B* **46**, 239 (1982).
- ¹⁷M. Bennett (unpublished).
- ¹⁸M. H. Brodsky, M. A. Frisch, J. F. Ziegler, and W. A. Lanford, *Appl. Phys. Lett.* **30**, 561 (1977).
- ¹⁹N. Maley, I. Szafranek, L. Mandrell, M. Katiyar, J. R. Abelson, and J. A. Thornton, *J. Non-Cryst. Solids* **114**, 163 (1989).
- ²⁰M. Katiyar, G. Feng, J. R. Abelson, and N. Maley, in *Amorphous Silicon Technology*, edited by A. Madan, Y. Hamakawa, M. J. Thompson, P. C. Taylor, and P. G. LeComber, MRS Symp. Proc. No. 219 (Materials Research Society, Pittsburgh, in press).
- ²¹N. Blayo and B. Drevillon, *J. Non-Cryst. Solids* **137&138**, 771 (1991).
- ²²Y. Toyoshima, K. Arai, A. Matsuda, and K. Tanaka, *J. Non-Cryst. Solids* **137&138**, 765 (1991).
- ²³H. Shanks, C. J. Fang, L. Ley, M. Cardona, F. J. Demond, and S. Kalbitzer, *Phys. Status Solidi B* **100**, 43 (1980).
- ²⁴P. John, I. M. Odeh, M. J. K. Thomas, M. J. Tricker, and J. I. B. Wilson, *Phys. Status Solidi B* **104**, 607 (1981).
- ²⁵S. Oguz, Ph.D. thesis, Harvard University, 1981. Oguz determined a proportionality factor between N_H and $\int \alpha dE$. We have converted this into a proportionality factor between N_H and $\int (\alpha/\omega)d\omega$, which is the more commonly used form.
- ²⁶W. E. Carlos and P. C. Taylor, *Phys. Rev. B* **25**, 1435 (1982).
- ²⁷J. B. Boyce and M. Stutzmann, *Phys. Rev. Lett.* **54**, 562 (1985).
- ²⁸M. Cardona, *Phys. Status Solidi B* **118**, 463 (1983).
- ²⁹H. R. Shanks, F. R. Jeffrey, and M. E. Lowry, *J. Phys. (Paris) Colloq.* **42**, C4-773 (1981).
- ³⁰*Handbook of Optical Constants of Solids*, edited by E. D. Palik (Academic, Orlando, FL, 1985).